



WEDNESDAY SLIDE CONFERENCE 2023-2024

Conference #10

15 November 2023

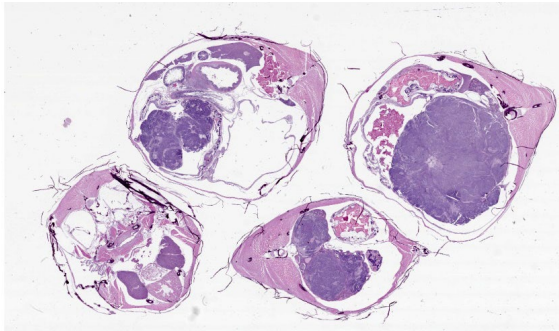


Figure 1-1. Transverse sections, betta. Sub-gross magnification demonstrates a large basophilic neoplasm occupying a large portion of the coelom. (HE, 5X)

CASE I:

Signalment:

Adult female betta fish, piscine (*Betta splendens*)

History:

This adult, female betta fish exhibited erratic and abnormal swimming behavior for 17.5 days. The owner described the fish as happy-go-lucky since being purchased at the local fish store. The fish even swam up to be caressed on the head at times. One day, after 2 years, the owner noted the fish had difficulty swimming. The owner also noticed that the fish had a greatly distended coelomic cavity. The fish was subsequently euthanized.

Gross Pathology:

There was an approximately 1 cm diameter distension of the coelomic cavity. On cut section, the mass was tan and solid.

Microscopic Description:

Kidney: Expanding and occupying greater than 90% of the coelomic cavity, compressing and displacing adjacent organs, and arising from the kidney, is a well-demarcated, unencapsulated, densely cellular, 0.75 cm diameter neoplasm composed of three distinct cell populations supported on a variably fine fibrovascular stroma. The first cell population is composed of polygonal cells (blastemal cells) which irregularly merge into two other populations. An epithelial cell population is arranged in palisading, branching, and tubule-like formations that often resemble lumens.

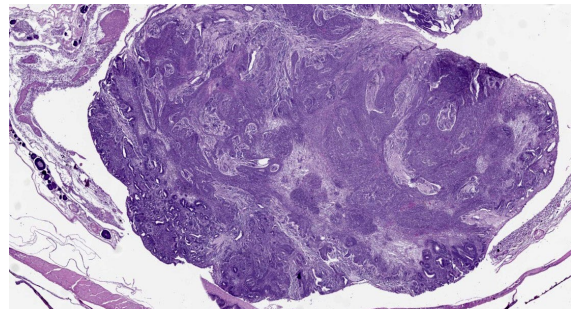


Figure 1-2. Coelom, betta. A large neoplasm is composed of multiple patterns including broad streams, bundles, and tubules. (HE, 36X)

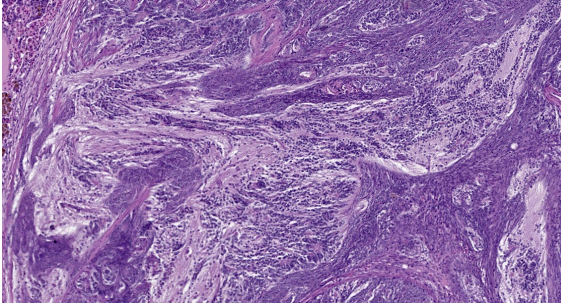


Figure 1-3. Coelomic mass, betta. The predominant cells are neuroectodermal and are occasionally embedded in neuropil. (HE, 183X)

The third population resembles small, compact tufts of cells (glomeruloid structures). Spindle to stellate cells are scattered throughout the neoplasm (embryonal mesenchyme). Polygonal blastemal cells have indistinct cell borders, a high nuclear to cytoplasmic ratio, a scant amount of eosinophilic cytoplasm, round to oval nuclei, and dense chromatin with indistinct nucleoli. Epithelial cells are cuboidal to columnar with variably distinct cell borders, a moderate amount of eosinophilic cytoplasm, round to oval nuclei with stippled chromatin and variably distinct nucleoli. Embryonal mesenchymal cells are spindle to stellate and loosely arranged, with indistinct cell borders, scant eosinophilic cytoplasm with elongate to oval nuclei and indistinct nucleoli. Mitotic figures are not present in the neoplasm. Peripherally, ova are multifocally degenerate and are atrophied with variably sized, irregularly shaped oocyte borders.

Transmurally and multifocally expanding the stomach wall are variably dense aggregates of macrophages interspersed with areas of spindle cells and fibrous connective tissue. Multifocally throughout the stomach wall and extending into the coelomic cavity are 40-100um diameter granulomas characterized by a core of brightly eosinophilic ne-

crotic debris, foamy macrophages, degenerate inflammatory cells, and mineral which are surrounded by variably dense concentric lamellations of spindle cells and macrophages. Multifocally, there are less developed granulomas that contain foamy macrophages with a light yellow-brown hemosiderin-like pigment. Scattered throughout the ovaries are multiple granulomas as previously described.

Contributor's Morphologic Diagnoses:

1. Betta fish, kidney: Nephroblastoma.
2. Betta fish, ovaries, stomach and coelomic cavity: Granulomas, multiple, most likely *Mycobacteria* spp.

Contributor's Comment:

Nephroblastoma is considered a common primary tumor of pigs, chicken, and fish with varying reports in dogs, cats, and cattle.⁷ In this case, spontaneous nephroblastoma in *Betta splendens* ("Siamese fighting fish") has been reported with other fish species, to include Japanese eels (*Anguilla japonica*), koi (*Cyprinus carpio*), and striped bass (*Morone saxatilis*).^{2,4,6,12} Nephroblastomas arise from neoplastic transformation of nephrogenic stem cells, which give rise to the characteristic blend of three cell populations that attempt to parallel the histo-anatomic components of the kidney through epithelial, blastemal, and mesenchymal cells. The cause of these

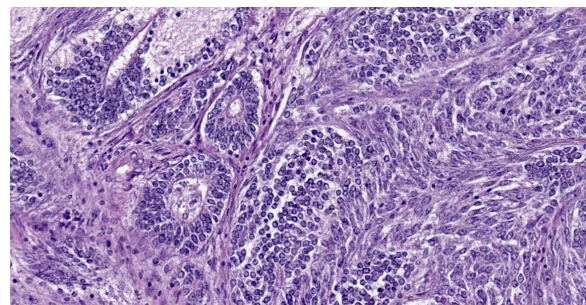


Figure 1-4. Neoplasm, betta. Rosettes are commonly seen in the neuroectomal tissue. (HE, 613X)

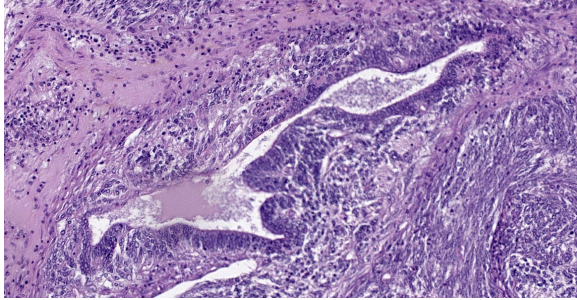


Figure 1-5. Neoplasm, betta. Columnar epithelium forms tortuous single-layered structures resembling gastrointestinal tissue. (HE, 363X)

tumors in fish is considered spontaneous, but has also been attributed to carcinogens.⁵ Other than coelomic enlargement, the clinical presentation of nephroblastoma in fish varies.

Mycobacteriosis affects wild and cultured freshwater, marine, and brackish fish worldwide, and frequently manifests as a chronic, progressive, and systemic disease.¹⁰ Transmission routes vary but may include cannibalism of infected fish, consumption of contaminated feed and/or detritus, or shedding from other aquatic vertebrates.

Although many *Mycobacteria* species have been isolated from fish, the most frequent and significant fish mycobacterioses include *M. chelonae*, *M. fortuitum*, and *M. marinum*.¹ Granuloma formation due to *Mycobacteria* infection in fish can be identified grossly (grayish-white, miliary nodules) and histologically in a variety of organs to include, but not limited to, the spleen, kidney, liver, and coelomic cavity. The histologic appearance of granulomas in most fish species is characterized by an outer wall of concentrically layered epithelioid macrophages, necrotic centers, and variable numbers of acid-fast bacilli within the core. The epithelial cell characteristics of these epithelioid macrophages is

demonstrated by positive immunoreactivity for cytokeratin.^{8,9}

The cause of death in this fish is most likely multi-factorial and attributed to pathophysiologic changes associated with tumor compression of vital organs and granuloma formation in multiple organs.

JPC Diagnosis:

1. Ovaries, posterior kidney, and coelom: Teratoma.
2. Ovaries: Follicular degeneration and necrosis, multifocal, chronic, moderate (follicular stasis/egg binding).
3. Stomach and coelom: Granulomatous and fibrosing gastritis, transmural, regionally extensive, severe, with regional coelomitis and intralesional birefringent debris (foreign body).

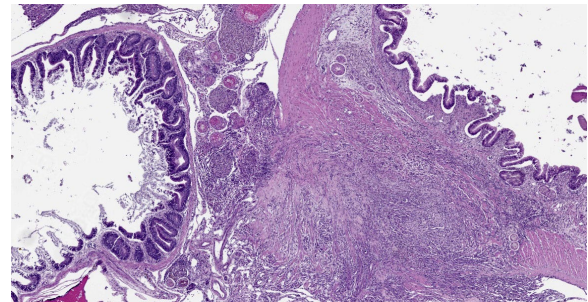


Figure 1-6. Stomach, betta. There is a focal fibrous adhesion between the stomach and a loop of bowel with embedded granulomas. (HE, 69X)

JPC Comment:

We agree with the contributor that there are three populations of cells within the examined section; however, we interpret these populations to originate from the three primordial germ layers, and thus prefer a diagnosis of teratoma. The examined section contains multiple large areas of neural differentiation (ectoderm), sheets of primitive mesenchymal tissue (mesoderm), and numerous tubular structures (endoderm). The teratoma

is adhered to and infiltrates both the posterior kidney and the ovary. Intracoelomic teratomas usually originate from the ovary in female fish, making ovarian origin most likely for this tumor.¹¹ As in this case, teratomas in fish often present as large coelomic masses causing coelomic distention.^{2,11}

While most cases of granulomatous inflammation in fish should be stained with acid fast stains to rule out mycobacteriosis, the distribution of granulomas in this case would be an unusual presentation. Mycobacteriosis in fish typically causes discrete granulomas or sheets of macrophages in the liver, spleen, kidney, skin, and coelom. In this case, infection and fibrosis track through the gastric wall in a manner most consistent with trauma (foreign body). The H&E slide was examined under polarized light and birefringent material was noted in the granulomas in the coelomic cavity adjacent to the gastric lesion, further supporting foreign body trauma. Acid fast stains were applied to the lesions and were negative.

We note the contributor's reference to granulomas in the ovaries; however, in our examined sections, these structures consist mostly of shrunken and necrotic ovarian follicles being engulfed by macrophages. This is a common lesion of follicular degeneration/egg binding and was likely caused by the mass effect of the teratoma preventing normal follicular release.

This week's conference was moderated by Dr. Elise LaDouceur, Chief of Extramural Projects and Research at the Joint Pathology Center. Conference participants were of two schools, with all participants diagnosing either nephroblastoma or teratoma. All participants were eventually convinced of teratoma by the large areas of neural differentiation and ciliated epithelium.

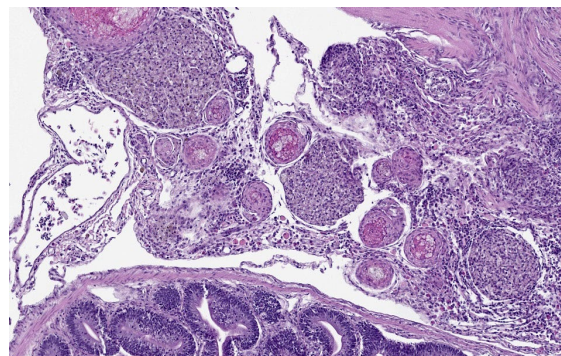


Figure 1-7. Omentum, beta. There are numerous well-formed granulomas within the omental adhesion. (HE, 186X)

Discussion also centered on whether the tumor was arising from or invading into the posterior kidney and ovary. While this was impossible to determine from the examined sections, in all species, teratomas most commonly arise in the gonads, making ovarian origin mostly likely.

Participants discussed egg binding, also known as follicular stasis. This condition in teleost fish has many causes, including mass effect, inflammation, or lack of access to nesting areas.

References:

1. Decostere A, Hermans K, Haesebrouck F. Piscine mycobacteriosis: a literature review covering the agent and the disease it causes in fish and humans. *Vet Microbiol.* 2004;99(3-4):159-166.
2. Groff JM. Neoplasia in fishes. *Vet Clin North Am Exot Anim Pract.* 2004;7(3):705-706.
3. Helmboldt CF, Wyand DC. Nephroblastoma in a striped bass. *J Wildl Dis.* 1971;7:162-165.
4. Lombardini ED, Law M, Lewis BS. Nephroblastoma in two Siamese fighting fish (*Betta splendens*). *Fish Pathol.* 2010;45:137-139.
5. Lombardini ED, Hard GC, Harshbarger JC. Neoplasms of the urinary tract in

- fish. *Vet Pathol.* 2014;51(5):1000-1012.
6. Masahito P, Ishikawa T, Okamoto N, et al. Nephroblastomas in the Japanese eel, *Anguilla japonica* Temminck et Schlegel. *Cancer Res.* 1992;52:2575–2579.
 7. Meuten DJ, Everitt J, Inskeep W, et al. *Histological classification of tumors of the urinary system of domestic animals.* Armed Forces Institute of Pathology; 2004.
 8. Noga EJ, Dykstra MJ, Wright JF. Chronic inflammatory cells with epithelial cell characteristics in teleost fishes. *Vet Pathol.* 1989;26(5):429-437.
 9. Polinas M, Padrós F, Merella P, et al. Stages of granulomatous response against histozoic metazoan parasites in mullets (Osteichthyes: Mugilidae). *Animals (Basel).* 2021;11(6):1501.
 10. Puk K, Guz L. Occurrence of *Mycobacterium* spp. in ornamental fish. *Ann Agric Environ Med.* 2020;27(4):535-539.
 11. Romanucci M, Arbuatti A, Massimini M, Defourny SP, Della Salda L. Ovarian teratoma in an adult female *Zoogoneticus tequila* (Webb & Miller 1998): histological and immunohistochemical features. *J Fish Dis.* 2017;40(6):859-862.
 12. Stegeman N, Heatley JJ, Rodrigues A, et al. Nephroblastoma in a koi (*Cyprinus carpio*). *J Exotic Pet Med.* 2010;19:29803.

CASE II:

Signalment:

1-year-old, female red abalone (*Haliotis rufescens*)

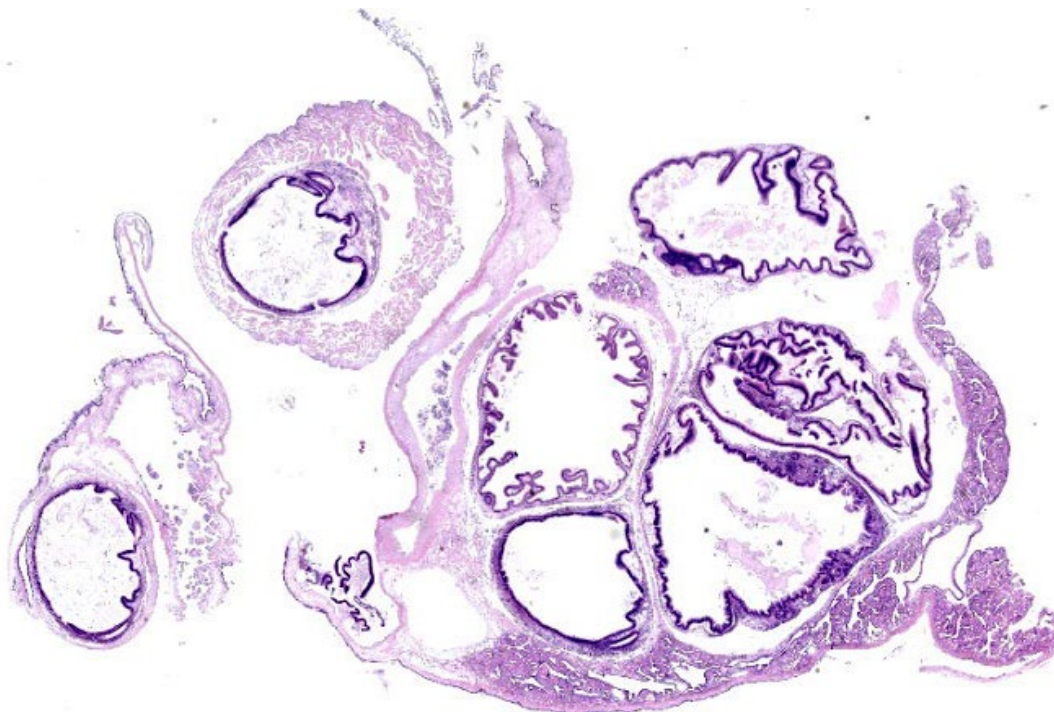


Figure 2-1. Transverse section, abalone. A transverse section of the body of an abalone (and two additional sections of gut) is submitted for examination with no lesions visible at this magnification. (HE, 5X)

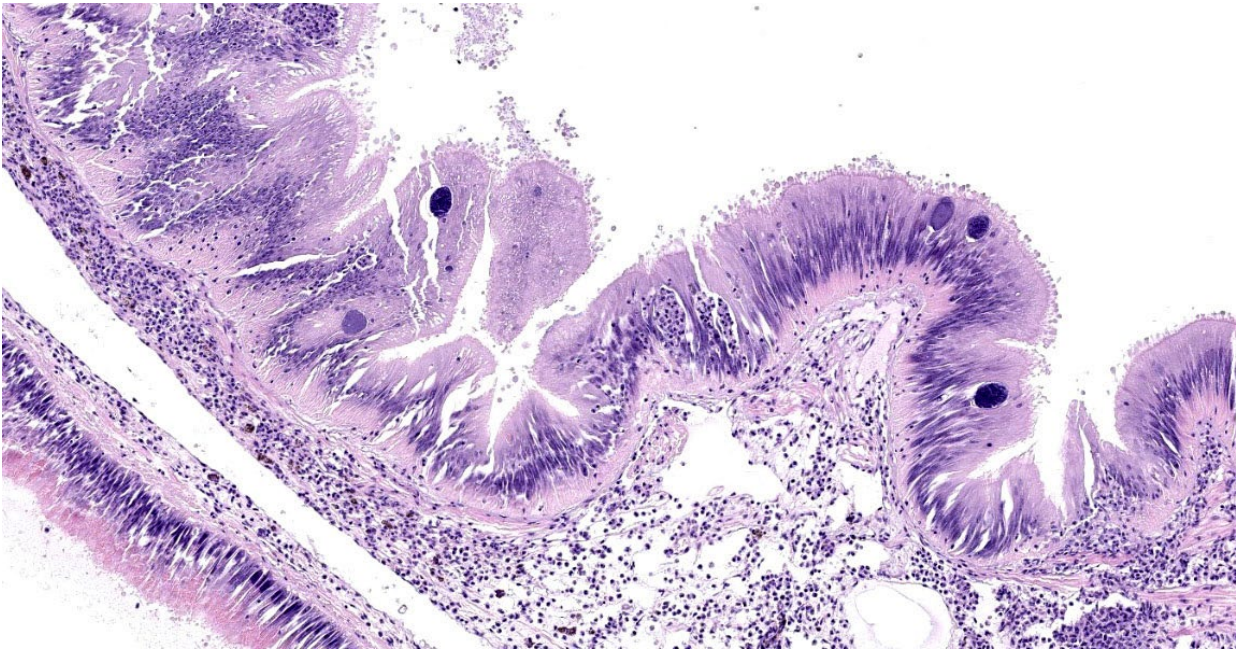


Figure 2-2. Gut, abalone. There are scattered epithelial cells which are markedly distended by a cytoplasmic vacuole containing numerous punctate bacilli. (HE, 137X)

History:

Four red abalone were acquired from California for placement in an aquarium. Receding tissues were noted in one of the animals. The co-housed animal was apparently healthy.

Laboratory Results:

PCR for *Xenohalotis californiensis* was positive.

Microscopic Description:

Posterior esophagus: Moderate numbers of epithelial cells lining the posterior esophagus contain large (15-20 μm in diameter) basophilic cytoplasmic inclusions. The inclusions range from palely basophilic and homogeneous to moderately basophilic and punctate to deeply basophilic and granular. The majority of inclusions are located in the apical aspect of the epithelial cells. Rarely, there are similar inclusions in the intestinal epithelium. Hucker-Twort gram stain shows the organisms within the inclusions to be gram negative.

Contributor's Morphologic Diagnosis:

Posterior esophagus: Moderate numbers of intracytoplasmic epithelial inclusions consistent with rickettsiae (abalone rickettsiosis).

Contributor's Comment:

Inclusions within the digestive tract of this animal are consistent with infection with the rickettsial organism *Xenohalotis californiensis*, the agent associated with abalone withering syndrome. As this disease is reportable to the OIE, samples were submitted to the NVSL for confirmatory histopathology and PCR testing. A PCR product generated with PCR primers proscribed by the OIE was sequenced and showed 99.37% identity with *X. californiensis* sequences in Gen Bank.⁴

Abalone withering syndrome affects multiple species within the *Halotis* genus in both wild and farmed animals. The causative agent, *Xenohalotis californiensis*, primarily infects the posterior esophagus and the digestive

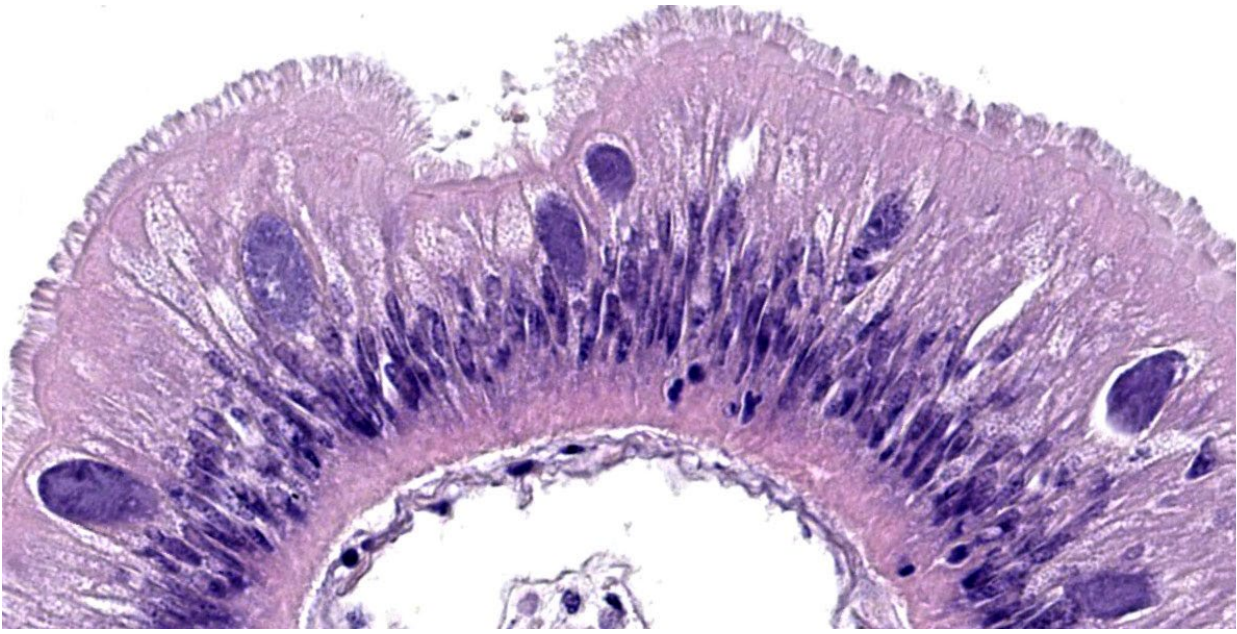


Figure 2-3. Gut, abalone. This field contains several infected intestinal epithelial cells with rickettsial inclusions at varying stages of maturity. (HE, 381X)

gland, but can also be seen to a lesser extent in the intestine.⁵ Some of the slides submitted here have rare cytoplasmic inclusions present in intestinal epithelial cells. Sections of the digestive gland from this animal are not present on the submitted slides; additional sections containing the digestive gland examined by the submitter did not exhibit inclusions within digestive gland cells. Infection of the digestive gland leads to degeneration/metaplasia of the digestive tubules which leads to anorexia, depletion of glycogen reserves, and subsequent use of the foot muscle as an energy source.⁵ Atrophy of the foot muscle is the characteristic gross change that gives the syndrome its name.

Contributing Institution:

USDA/APHIS
 NVSL Pathology Laboratory
https://www.aphis.usda.gov/aphis/ourfocus/animalhealth/lab-info-services/sa_about_nvsl/ct_about_nvsl

JPC Diagnosis:

1. Gut: Epithelial necrosis, single cell, multifocal, moderate, with hemocytic inflammation and intracytoplasmic bacterial inclusions.
2. Kidney: Coccidiosis, intraepithelial, multifocal, moderate with mild epithelial degeneration.

JPC Comment:

Withering syndrome (WS) is a bacterial disease characterized by a severely shrunken body and infection by the organism *Xenohaliotis californiensis*. The organism is an obligate intracellular bacterium that infects the abalone digestive epithelia, causing the morphologic abnormalities detailed by the contributor and resulting in physiologic starvation.¹ The organism is likely spread via direct fecal-oral transmission, with initial infection in the post-esophagus, followed by the intestine, and finally and most devastatingly, the digestive gland.¹

WS affects all members of the *Haliotis* genus with varying degrees of severity, depending

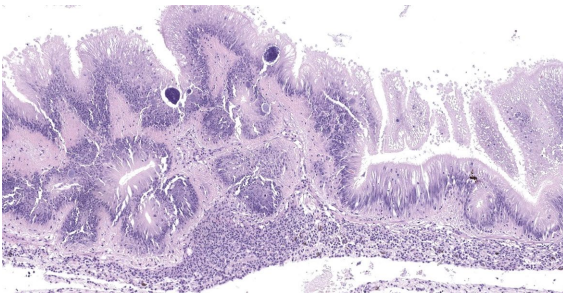


Figure 2-4. Gut, abalone. There are numerous hemocytes infiltrating the spongy connective tissue adjacent to the affected sections of gut. (HE, 317X)

on species and environmental conditions. The disease was first observed in black abalone populations on the California coast in 1985 after a particularly strong El Niño event caused sustained, increased water temperatures off the western US.¹ This pattern has held in subsequent years, with the geographic range of clinical WS moving steadily ever northward with increasing coastal water temperatures and episodic high-mortality events associated with El Niño years.

Temperature is the central factor in the ecology of WS with transmission and disease nearly eradicated at water temperatures of 12.3°C, but high transmission and extreme clinical signs evident at 18.7°C.¹ The susceptibility of *Haliotis* species also varies widely, with green and pink abalone exhibiting no clinical effects of infection and no mortality, red abalone exhibiting moderate mortality, and black abalone exhibiting catastrophic mortality rates of up to 99%.¹

Diagnosis of WS requires both identification of the pathogen, either by *in situ* hybridization or by PCR and sequence analysis, and observation of the characteristic histologic changes of pedal and digestive gland atrophy and digestive gland metaplasia. PCR may also be used to detect *Xenohaliotis californiensis* prior to the movement of animals as part of infectious disease prevention protocols.¹ Scrupulous husbandry practices,

such as reduced stocking densities, maintaining cool water temperatures, disinfection of hands and equipment when moving among groups or tanks of animals, and isolation or culling of infected animals are the mainstays of WS prevention in *Haliotis* species under human care.

Despite the dramatic mass mortality events associated with WS, certain black abalone populations appear to have developed some resistance to the disease, with progeny of mass mortality event survivors experiencing longer survival times upon infection.² In a second optimistic development, a bacteriophage has been identified within *Xenohaliotis californiensis* in WS-affected farmed abalone. The presence of this bacteriophage effectively eliminates the ability of *Xenohaliotis californiensis* to cause disease in farmed abalone, though the extent to which the phage is present in the wild is currently unknown.² More research is currently needed to understand the complex interactions of climate change, water temperatures, natural selection pressures, and host-agent-parasite relationships and what these interactions portend for the future of *Haliotis* species.

Conference participants briefly discussed the anatomy and ecology of the red abalone, which, due to their endangered status, can only be harvested via recreational free diving. Participants also discussed the coccidial organisms noted throughout the kidney. These are most consistent with *Margolisiella haliotis* (formerly called *Pseudoklossia haliotis*; also called, rather pointedly, abalone kidney coccidia) which infects multiple species of abalone and targets renal epithelial cells. Lesions reportedly associated with this infection include renal epithelial cell hypertrophy and inflammation.³

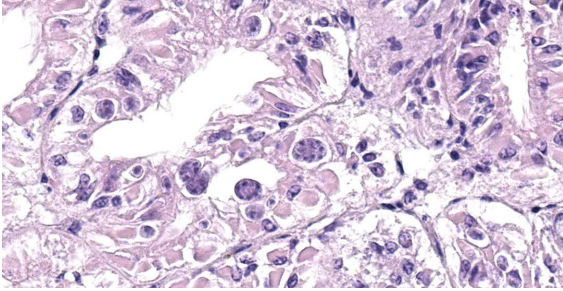


Figure 2-5. Renal papilla, abalone. There are numerous apicomplexan meronts and schizonts within the epithelium of the renal papilla. (HE, 391X)

Participants discussed lesion localization within the abalone digestive tract. The moderator felt it unnecessary to parse the different gastrointestinal segments present on the examined slide, particularly since the term “gut” is used extensively in invertebrate pathology to refer to the entire invertebrate tubular alimentary tract. Discussion ended with a quick review of rickettsia-like bacterial diseases of veterinary note, including *Epitheliocystis*, *Rickettsiella scorpionisepticum*, *Neorickettsia risticii*, and *Neorickettsia helmintheca*.

References:

1. Crosson LM, Wight N, VanBlaricom GR, Kiryu I, Moore JD, Friedman CS. Abalone withering syndrome: distribution, impacts, current diagnostic methods and new findings. *Dis Aquat Org.* 2014;108:261-270.
2. Friedman CS, Wight N, Crosson LM, VanBlaricom GR, Lafferty KD. Reduced disease in black abalone following mass mortality: phage therapy and natural selection. *Front Microbiol.* 2014;5:1-10.
3. Friedmann CS, Gardner GR, Hedrick RP, Stephenson MD, Cawthorn RJ, Upton SJ. *Pseudoklossia haliotis* sp. n. (Apicomplexa) from the kidney of California abalone, *Haliotis* spp. (Mollusca). *J. Invertebr. Pathol.* 1995;66:33-38.

4. World Health Organization. Chapter 2.4.8 *Infection with Xenohaliothis californiensis* In: *Aquatic Animal Health Code.* 2019:8-9.
5. World Health Organization. Chapter 2.4.8 *Infection with Xenohaliothis californiensis* In: *Aquatic Animal Health Code.* 2019:2-3.

CASE III:

Signalment:

Juvenile, male Harbour porpoise, cetacean (*Phocoena phocoena*)

History:

This animal was found dead on the beach.

Gross Pathology:

There was white frothy material in the trachea which extended to just proximal to the tracheal bifurcation (mild to moderate pulmonary oedema). There was a moderate amount of white frothy material in the primary bronchi (pulmonary oedema). There were myriad, large (approx. 6 cm long and 1 mm diameter) nematodes within the primary, secondary and tertiary bronchi.



Figure 3-1. Lung, porpoise. Secondary bronchi contain numerous nematodes. (Photo courtesy of: The University of Liverpool, <https://www.liverpool.ac.uk/veterinary-science/>)



Figure 3-2. Lung, porpoise. Pulmonary froth has washed several nematodes up into the proximal trachea. (Photo courtesy of: The University of Liverpool)

In the smaller bronchi the lumens were frequently filled with nematodes. The right lung was diffusely slightly darker red than the left (hypostasis). The left lung exhibited several parallel dark and light red stripes (rib imprints). Throughout the lung parenchyma, bilaterally, there were multiple firm foci ranging from 5 to 15 mm diameter, which were red to cream on cut surface, and sometimes contained nematodes (severe verminous pneumonia). Other lesions included: gastritis, multifocal, subacute, moderate, with intralésional nematodes and mucosal ulceration; inner ear, nematodiasis, bilateral, subacute, moderate to severe; abdominal cavity, haemoperitoneum, acute, diffuse, mild to moderate; mesenteric lymph nodes, lymphadenomegaly, diffuse, subacute, moderate; skin, abrasion, multifocal, acute, mild to moderate; liver, scar, multifocal, chronic, minimal.

Laboratory Results:

Lung: Light growth of *Salmonella* spp. obtained from cultures.

Microscopic Description:

Two sections of lung: Multiple secondary and tertiary bronchi contain multiple intraluminal 1 mm diameter nematodes characterised by the presence of a 15 μ m thick cuticle, coelomyarian musculature, and lateral cords. Bronchi also contain immature individuals and embryonated eggs, as well as degenerated sloughed epithelial cells and extravasated erythrocytes (haemorrhage). There is moderate diffuse infiltration of eosinophils and fewer lymphocytes, plasma cells and macrophages in the epithelium and lamina propria of the affected bronchi.

Approximately 50% of the section examined is effaced by multifocal to coalescing accumulations of a dense light eosinophilic material surrounded by elongated cells (fibroblasts), foreign body type multinucleated giant cells (up to 20 nuclei) and epithelioid macrophages (granulomas). These areas occasionally contain a moderate to large amount of eosinophilic to basophilic angular to crystalline material (mineralisation).

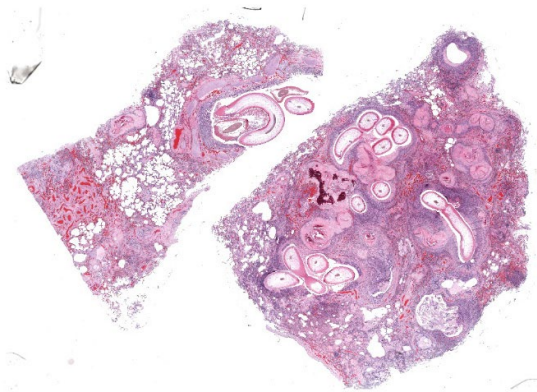


Figure 3-3. Lung, porpoise. At subgross magnification, numerous nematodes can be seen within airways. The alveolar parenchyma is largely effaced by fibrosis and inflammation. (HE, 5X)



Figure 3-4. Lung, porpoise. Cross and tangential sections of larval nematodes are present within a bronchiole. The adjacent airway epithelium is markedly hyperplastic, inflamed, and fibrotic. (HE, 23X)

Multifocally, bronchioles and alveoli are filled with a moderate to large amount of necrotic cellular debris, a moderate number of eosinophils, macrophages with foamy cytoplasm, lymphocytes, light eosinophilic amorphous material (oedema), light eosinophilic fibrillary material (fibrin) and, occasionally, 0.5 μm maximum length extracellular basophilic coccobacilli. These areas are often associated with the presence of thin-walled cysts (up to 1.5 mm diameter) within the parenchyma, which contain multiple small (200 μm diameter) nematodes in both transverse and longitudinal section. These nematodes have a 5-10 μm cuticle with coelomyarian musculature, and lateral cords. The coelom contains an intestinal tract and reproductive tract with larvae. There is also a mixed inflammatory infiltration on the alveolar wall, composed of eosinophils, lymphocytes and plasma cells and multifocal areas of dark basophilic angular to crystalline material (mineralisation).

Pulmonary arteries show marked smooth muscle hyperplasia with reduction of the arterial lumen. Alveolar capillaries show proliferation and congestion. There are also areas of atelectasis and alveolar distension with rupture of alveolar wall (emphysema).

Contributor's Morphologic Diagnosis:

Lung: Bronchopneumonia, granulomatous and eosinophilic, multifocal, chronic, severe, with intralesional nematodes, fibrosis and mineralisation.

Contributor's Comment:

The histological features represent a case of granulomatous and eosinophilic bronchopneumonia associated with lungworms in a harbor porpoise. In the present case, *Salmonella enterica* Group B has also been isolated from the pulmonary lesions and is likely to be a clinically significant finding.

Lungworms are a common finding in wild cetaceans, with species of nematodes reported in up to 69% of stranded Harbour porpoises (*Phocoena phocoena*), all from the family *Pseudaliidae*.^{6,7} *Pseudalius inflexus* and *Torynurus convolutus* are found in the bronchi, bronchioles and blood vessels, whereas *Halocercus invaginatus* inhabits the pulmonary parenchyma.^{2,9}



Figure 3-5. Lung, porpoise. A cross section of the large nematode larva in the airway has a thin cuticle with irregularly spaced cuticular ridges, polymyarian-coelomyarian musculature, and a central small intestine with uninucleate cells with cytoplasmic hematin pigment. There is no evidence of gonads. (HE, 92X)

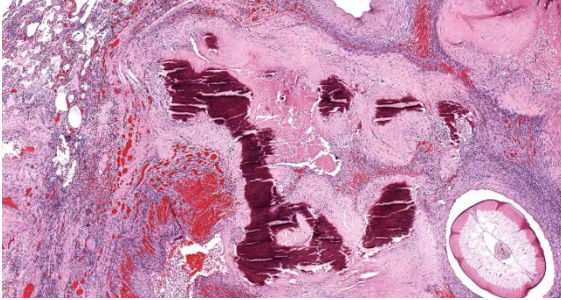


Figure 3-6. Lung, porpoise. Some airways are largely occluded by fibrosis and mineralization. (HE, 37X)

In this case, it appears most likely that the nematodes in the upper airways and the bronchioles were *P. inflexus* and *T. convolutus* and those within the parenchyma were *H. invaginatus*.

Verminous pneumonia is a common finding although is not frequently thought to be the primary cause of death. However, there can be severe changes, resulting in extensive fibrosis and mineralisation, as seen in this case. There is evidence that increased parasitic burden is associated with high levels of pollutants (polychlorinated biphenyls) which are associated with immunosuppression.³ In addition, some studies suggest that lungworms may act as a potential means of transfer of bacterial infections in harbour porpoise, with *Salmonella enterica* Group B, as cultured in the current case, identified as potentially spread in this way.⁴⁻⁶ The case presented here reinforces the theory that parasites should be considered as potential vectors of zoonotic bacterial infections in marine mammals.

Contributing Institution:

The University of Liverpool
<https://www.liverpool.ac.uk/veterinary-science/>

JPC Diagnosis:

1. Lung: Bronchopneumonia, eosinophilic, multifocal, with intrabronchial metastrongyle nematodes.
2. Lung: Pneumonia, interstitial, eosinophilic, multifocal, chronic, severe, with intraparenchymal adult metastrongyle nematodes.
3. Lung: Pneumonia, interstitial, eosinophilic, multifocal severe, with intraparenchymal nematodes.

JPC Comment:

This case provides an excellent example of lungworm parasitism in a harbour porpoise, a marine species found in the North Atlantic Ocean that typically bears a heavy pulmonary parasite burden.³ Studies of the harbour porpoise have found that parasites are most common in the respiratory system, and lungworms have been found in virtually all harbour porpoises older than 1 year, most often in the bronchial tree and the pulmonary blood vessels.⁹ As in this case, parasites within the pulmonary parenchyma typically incite an eosinophilic and granulomatous bronchointerstitial pneumonia. When found in the pulmonary blood vessels, nematodes can cause chronic thrombosis and vasculitis, often with calcification of thrombotic material.⁹

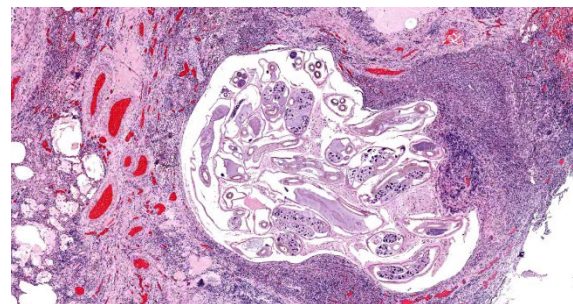


Figure 3-7. Lung, porpoise. A second, much smaller nematode is present within the alveolar parenchyma. (HE, 32x)

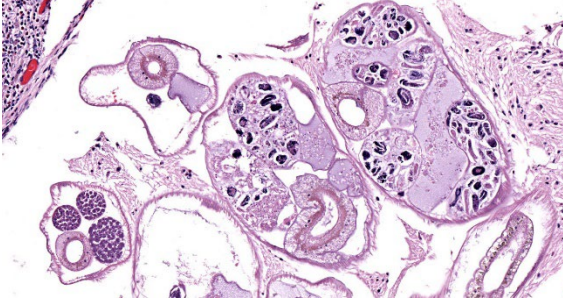


Figure 3-8. Lung, porpoise. Cross sections of adult male and female metastrongyles. At left is a smaller male with three cross-sections of a sperm-laden testes. Larger cross sections are of female worms with characteristic “larvated” metastrongyle eggs (and some embryonated eggs as well) within their uteri. (HE, 185X)

In general, far less is known about the biology of pulmonary parasites of marine mammals compared to their terrestrial counterparts; however, two of the nematodes examined here belong to the metastrongyle family which, collectively, are far less mysterious. Metastrongyles, or “lungworms,” have coelomyarian musculature, an external cuticle that is typically smooth, an intestine lined by few multinucleated cells, and accessory hypodermal cords. Mature females can produce either eggs or fully developed embryos; species that produce eggs deposit them into host tissues where they embryonate.¹⁰ Other notable metastrongyles of veterinary importance include *Angiostrongylus cantonensis* (rat), *Dictyocaulus viviparus* (ruminants), *Muellerius capillaris* (small ruminants), *Metastrongylus apri* (pigs), *Aelurostrongylus abstrusus* (cats), and *Filaroides hirthi* (dogs).

This case incited robust discussion among conference participants. Participants identified three different nematode species in section: the large nematodes within the airways and two, much smaller nematode species within the parenchyma. Some participants remarked that many areas identified initially as

granulomas could represent foci of severe vasculitis, possibly secondary to intravascular lungworms. Of the three nematodes identified in section, participants felt that the smallest of the three, which were approximately 60um in diameter, had features consistent with filarid parasites, which could account for the possible vasculitis. Post-conference consultation with Dr. Christopher Gardiner confirmed that these nematodes are consistent with filarid nematodes, though we were unable to speciate them with the minimal features present in section.

The two largest nematodes in section are metastrongyles and contain very nice examples of the classic metastrongyle morphologic features described above. The largest nematodes are over 1mm in diameter and are morphologically consistent with *Pseudalius inflexus*; however, the lack of gonads within the examined section did not allow for definitive speciation. Interestingly, there are reports of *Pseudalius inflexus* causing similar lesions in Burmeister’s porpoises; those cases were accompanied by vasculitis and thrombosed arteries with a morphologic appearance similar to many of the presumptive occlusive vascular changes in this section.¹

Finally, the mid-sized nematode population, with a diameter of approximately 225um, contain classic metastrongyle features and female gonads contain developing larvae (see Figure 3-8). Similar to the previously discussed nematodes, we were unable to speciate these metastrongyles, though the species discussed by the contributor appear to be the most common causes of marine mammal pulmonary nematodiasis.

Conference participants debated combining the morphologic diagnoses or creating separate diagnoses based on etiology. As the three different nematodes each had different pathologic effects, participants preferred separate

morphologic diagnoses. And while participants felt strongly that a significant vasculitis was evident in the examined section, vasculitis was not included in the diagnosis due to the inability to confirm vasculitis with immunohistochemical stains on this entirely digital submission.

References:

1. Alvarado-Rybak M, Toro F, Abarca P, Paredes E, Espanol-Jimenez S, Seguel M. Pathological findings in cetaceans sporadically stranded along the Chilean coast. *Front Mar Sci.* 2020;7.
2. Balbuena JA, Aspholm PE, Andersen KI, Bjorge A. Lung-worms (Nematoda: Pseudaliidae) of harbour porpoises (*Phocoena phocoena*) in Norwegian waters: patterns of colonization. *Parasitology.* 1994;108:343-349.
3. Bull JC, Jepson PD, Sauna RK, et al. The relationship between polychlorinated biphenyls in blubber and levels of nematode infestations in harbour porpoises, *Phocoena phocoena*. *Parasitology.* 2006; 132:565-573.
4. Davison N, Barnett J, Rule B, Chappell S, Wise G. Group B *Salmonella* in lung-worms from a harbour porpoise (*Phocoena phocoena*). *Vet Rec.* 2010; 167:351-352.
5. Davison NJ, Simpson VR, Chappell S, et al. Prevalence of a host-adapted group B *Salmonella enterica* in harbour porpoises (*Phocoena phocoena*) from the southwest coast of England. *Vet Rec.* 2010; 167: 173-176.
6. Foster G, Patterson IA, Munro DS. Monophasic group B *Salmonella* species infecting harbour porpoises (*Phocoena phocoena*) inhabiting Scottish coastal waters. *Vet Microbiol.* 1999;65: 227-231.
7. Jepson PD, Baker JR, Kuiken T, Simpson VR, Kennedy S, Bennett PM. Pulmonary pathology of harbour porpoises (*Phocoena phocoena*) stranded in England and Wales between 1990 and 1996. *Vet Rec.* 2000;146:721-728.
8. Reckendorf A, Everaarts E, Bunskoek P, et al. Lungworm infections in harbour porpoises (*Phocoena phocoena*) in the German Wadden Sea between 2006 and 2018, and serodiagnostic tests. *Int J Parasitol Parasites Wildl.* 2021;14: 53-61.
9. Siebert U, Wunschmann A, Weiss R, Frank H, Benke H, Frese K. Post-mortem findings in harbour porpoises (*Phocoena phocoena*) from the German North and Baltic Seas. *J Comp Pathol.* 2001;124: 102-114.
10. Gardiner CH, Poynton SL. *An Atlas of Metazoan Parasites in Animal Tissues.* Armed Forces Institute of Pathology;2006.

CASE IV:

Signalment:

Hatch-year, female bald eagle, avian (*Haliaeetus leucocephalus*)



Figure 4-1. Liver, bald eagle. The liver was markedly enlarged (weighing 149g) and discolored brown to green with numerous pinpoint, beige, poorly-defined foci. (Photo courtesy of: Veterinary Diagnostic Laboratory, University of Minnesota, St Paul, MN. <https://vdl.umn.edu/>)

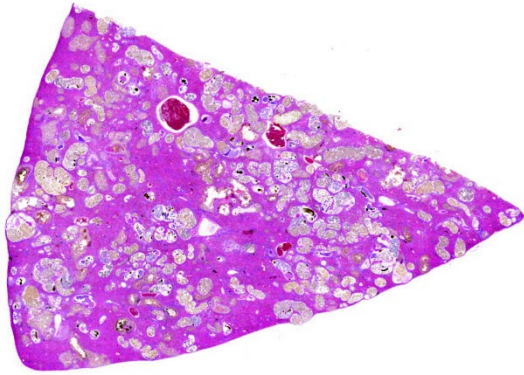


Figure 4-2. Liver, bald eagle. One section of liver is submitted for examination. At sub-gross magnification, numerous areas of palor are scattered throughout the section. (HE, 6X)

History:

The animal was emaciated. It was euthanized at admission to the wildlife clinic with suspected West Nile disease (neurologic signs and eye lesions consistent with chorioretinitis) and liver enlargement.

Gross Pathology:

The liver was markedly enlarged (weighing 149g) and discolored brown to green with numerous pinpoint, beige, poorly defined foci. Numerous fragile thin-walled parasites (flukes) less than 5.0 mm long were embedded in the liver.

Laboratory Results:

A liver sample tested positive for *Erschoviorchis* sp. by PCR and sequencing.

Microscopic Description:

Approximately 75% of the liver section is infiltrated by myriad metazoan parasites that have a thin, smooth tegument, a variably discernible ventral sucker, and numerous intraparenchymal, golden, operculated eggs that are approximately 25.0 x 12.0 μm (morphologically consistent with adult trematodes).

Hepatic cords are often dissociated, and sinusoids are frequently expanded by either brown to black fluke pigment, ova, fibrin, and/or numerous lymphocytes, heterophils, and macrophages, including multinucleated cells. Small numbers of lymphocytes, macrophages, and heterophils frequently surround trematodes and occasionally form small granulomas that are centered on areas of lytic necrosis.

Contributor's Morphologic Diagnosis:

Liver: Granulomatous hepatitis, multifocal to coalescing, moderate, chronic with numerous intraparenchymal adult trematodes.

Contributor's Comment:

Hepatic trematodosis is a sporadically reported disease in raptors, with a predominance for species in the *Opisthorchiidae* family. *Opisthorchis* sp., *Metorchis bilis*, and *Amphimerus elongatus* are all members of the *Opisthorchiidae* family and have been implicated in the previous cases of hepatic trematodosis of eagles. However, recently, a fluke of the genus *Erschoviorchis* has been reported to cause severe liver infections in bald eagles in the upper Midwest of the United States.^{3,5} Until recently, the only species within this genus was *E. lintoni*, which infects the pancreas of the common loon (*Gavia immer*) in North America.¹ *E. anuiensis*, the other species within this genus, was described from experimental infections of Muscovy ducks using metacercaria recovered from fish from the Amur River basin in the Russian Far East.⁴ Whether the *Erschoviorchis* sp. affecting the bald eagles was newly introduced to the United States or has long been established in North America and possibly confused with *Amphimerus elongatus* remains unknown.

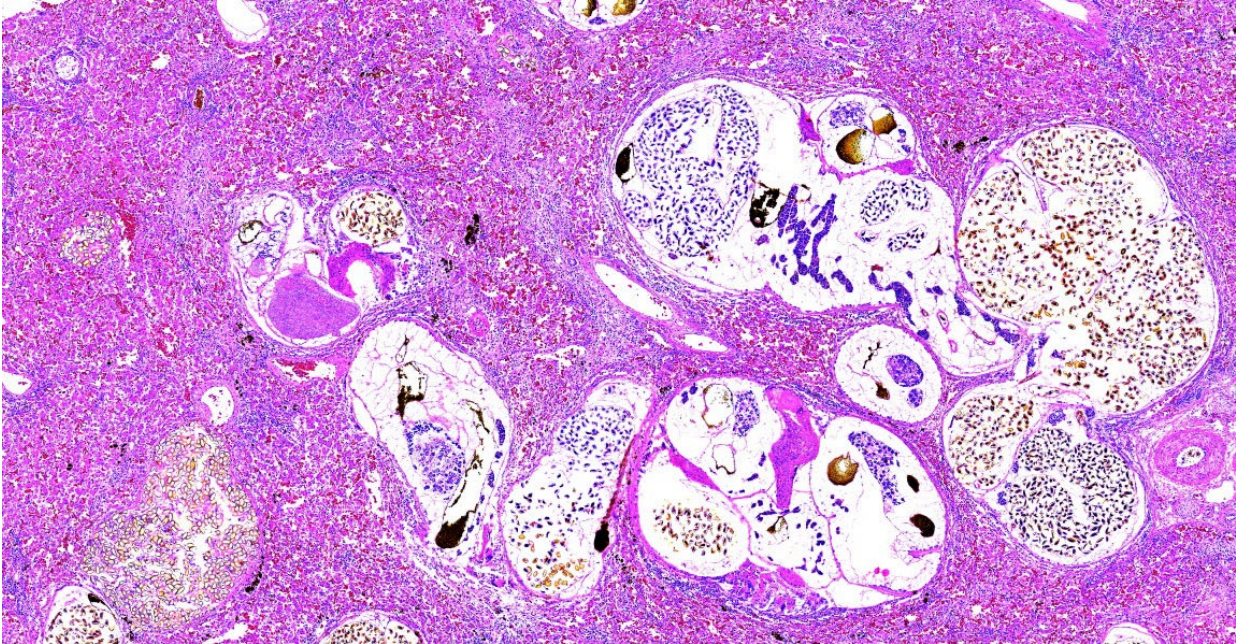


Figure 4-3. Liver, bald eagle. Numerous flukes are embedded within the hepatic parenchyma. (HE, 46X)

Erschoviorchis flukes are notoriously difficult to tease out from the affected tissue due to their fragile nature. As a result, the parasitological features described in this case are based on fluke fragments. Recovering complete flukes would be necessary to assign a new species denomination.

The life cycle of opisthorchiid flukes includes two intermediate hosts, typically a snail and a fish as the first and second host, respectively. Adult trematodes release eggs that are passed in the feces. The first intermediate host, a gastropod snail, ingests the eggs, which then release miracidia. These miracidia undergo several stages of development within the snail: sporocyst→rediae→cercariae. Cercariae are released from the snail and encyst in the skin or muscle of freshwater fish, the second intermediate host, to become metacercariae. The definitive host becomes infected by ingesting the raw, metacercariae-laden fish. Metacercariae generally excyst within the upper gastrointestinal tract of the definitive host and ascend to the

biliary ducts where they develop into adults.² The exact life cycle of this *Erschoviorchis* sp. is uncertain, but likely is similar to that of other opisthorchiid flukes.

Although *E. anuiensis* appears to be highly pathogenic based on experimental infections, the clinical significance of massive hepatic trematodosis in this case remains uncertain since West Nile virus infection was considered to be the more important disease problem. Co-infections of bald eagles with *Erschoviorchis* sp. liver flukes with West Nile virus appear to be common.³

Contributing Institution:

Veterinary Diagnostic Laboratory
University of Minnesota, St Paul, MN
<https://vdl.umn.edu/>

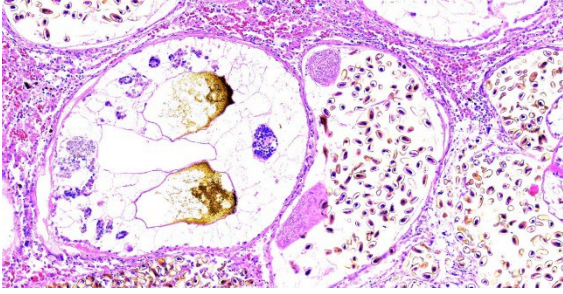


Figure 4-4. Liver, bald eagle. Cross sections of multiple trematodes demonstrate key characteristic diagnostic features for trematodes (it is difficult to find a single trematode that has all of them in section). Key characteristic features are a spongy body cavity, paired ceca (brown due to the presence of hematin), scattered vitellarian glands (on fluke at left), two cross sections of one or more suckers, and cross sections of a uterus with eggs. (HE, 46)

JPC Diagnosis:

Liver: “Extrematodiasis”. 😊

JPC Comment:

The contributor provides an excellent summary of *Erschiviorchis* sp. parasitism and the discovery of a potentially new pathogen of bald eagles in the upper Midwest of the United States.

In general, trematodes can be identified histologically by the following key histologic features: an oral sucker, paired ceca, no body cavity, spongy parenchyma, vitelline (yolk-forming) glands, hermaphroditism, and, with few exceptions, the presence of operculated eggs. Some common trematodes of veterinary importance include *Fasciola hepatica* in the bile ducts and gallbladder of ruminants, *Fascioloides magna* in the liver of certain wild ruminants, *Paragonimus kellicotti* in the lungs of dogs and cats, and *Heterobilharzia americanum* in dogs and some wildlife.

Conference discussion focused largely on the stunning appearance of the examined section, with eggs and adult trematodes in seemingly every micrometer of the tissue. Participants struggled to characterize the severity of the parasitism in this section, with “massive” and “extreme” being popular modifiers. Participants settled on a morph of “Liver: Trematodiasis, multifocal, extreme, with moderate, multifocal necrosis and granulomatous inflammation.” Disappointment was palpable in the room, however, as many felt that this rather quotidian diagnosis failed to capture the full glory of this gorgeous histologic specimen. Our cheeky JPC diagnosis was suggested by an eagle-eyed resident with a love of puns, and, once suggested, “Extrematodiasis” quickly soared to the top. We shall return to normal professional standards next wee (perhaps); in the meanwhile, the contributor provides an excellent morphologic diagnosis, as do we, buried midway through the paragraph above.

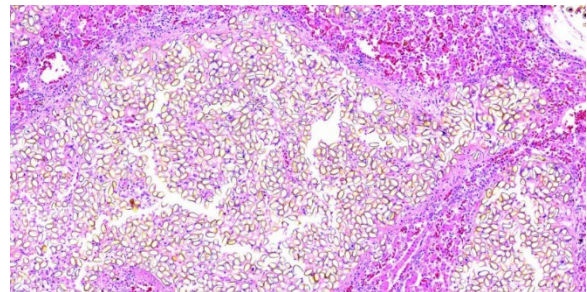


Figure 4-5. Liver, bald eagle. Aggregates of free eggs are present in the hepatic parenchyma. (HE, 137X)

References:

1. Gower WC. A new trematode from the loon, *Gavia immer*, and its relationship to *Haematotrephus fodiens* Linton, 1928. *Proc US National Museum* 1939;87:139–143.
2. King S, Scholz T. Trematodes of the family *Opisthorchiidae*: a minireview. *Korean J Parasitol* 2001;39:209–221.

3. McDermott KA, Greenwood SJ, Conboy GA, Franzen-Klein DM, Wünschmann A. Massive hepatic trematodosis in 5 juvenile bald eagles. *J Vet Diagn Invest.* 2023;35(4):409-412.
4. Tatonova YV, Besprozvannykh VV, Katugina LO, Solodovnik DA, Nguyen HM. Morphological and molecular data for highly pathogenic avian parasite *Erschoviorchis anuiensis* sp. n. and phylogenetic relationships within the *Opisthorchiidae* (Trematoda). *Parasitol Int* 2020; 75:102055.
5. Wünschmann A, Armien AG, Hoefle U, Kinne J, Lowenstine LJ, Shivaprasad HL. Birds of Prey. In: Terio KA, McAloose D, St. Leger J, eds. *Pathology of Wildlife and Zoo Animals*. Elsevier;2018:738.